

## Promoting the oxidative removal rate of 4-chlorophenol on gold-doped TiO<sub>2</sub>/graphene photocatalysts under UV light irradiation

V. I. Iliev\*, D. V. Tomova, V. F. Georgiev, S. K. Rakovsky

*Institute of Catalysis, Bulgarian Academy of Sciences, Acad. G. Bonchev St., Bldg. 11, 1113 Sofia, Bulgaria*

Submitted November 7, 2016; Revised February 2, 2017

4-Chlorophenol photooxidation catalysed by nanosized TiO<sub>2</sub>, Au/TiO<sub>2</sub>, and matching composite materials with reduced graphene oxide (GR) has been studied upon irradiation with UV light. XPS and TEM methods have been applied to characterise prepared photocatalysts. The average size of the titania nanoparticles prepared by the sol-gel method was 20 nm. TiO<sub>2</sub> and Au/TiO<sub>2</sub> particles were randomly distributed on the surface of the graphene nanosheets. The average size of the Au nanoparticles in the modified titania photocatalysts was about 7 nm. XPS measurements confirmed partial thermal reduction or photoreduction of the graphene oxide to graphene. Rate constants of 4-chlorophenol photooxidation catalysed by the studied samples followed the order: Au/TiO<sub>2</sub>/GR > Au/TiO<sub>2</sub> > TiO<sub>2</sub>/GR > TiO<sub>2</sub>. The rate constant of 4-chlorophenol degradation catalysed by an Au/TiO<sub>2</sub>/GR composite was approximately 3.9 times higher than that registered with titania. Enhanced activities of Au/TiO<sub>2</sub>/GR, Au/TiO<sub>2</sub>, and TiO<sub>2</sub>/GR photocatalysts were due to efficient charge carrier separation of the light-generated electron-hole pairs in titania semiconductor. This favoured an additional generation of HO• radicals on the titania valence band.

**Keywords:** photocatalysis, TiO<sub>2</sub>/graphene, Au/TiO<sub>2</sub>/graphene, graphene-semiconductor composite, 4-chlorophenol.

### INTRODUCTION

Photocatalytic reactions over semiconductor materials irradiated with solar or artificial light are of great interest because of their ability to remove a large variety of pollutants in both aqueous and gaseous phase [1,2]. Among various semiconductor photocatalysts, titanium dioxide (TiO<sub>2</sub>) is the most prevalent material for environmental applications [1]. However, a major disadvantage in most semiconductor materials is the high degree of recombination between the photogenerated charge carriers, which ultimately decreases the photocatalyst effectiveness and the photonic efficiency of the redox process. In the case of noble metal modified photocatalysts [3,4] the lifetime of the photogenerated pairs is increased due to efficient separation of the electron-hole charges generated upon irradiation.

In recent years graphene oxide (GO) and reduced graphene oxide (GR) have been used in the design of photocatalysts as a tool for improving the photocatalytic performance of the latter [5–9]. Results from these studies indicate that graphene is an excellent co-catalyst to enhance photocatalytic oxidation and reduction activity. Based on its excellent electron mobility, it is generally believed that graphene can rapidly separate and transfer photogenerated electrons and thus the electron-hole recombination process is impeded [5–8]. Moreover, as a result of  $\pi$ - $\pi$  interactions and formation of hydrogen bonds between organic pollutants and GO

or graphene the local concentration of polluting compounds around the investigated photocatalysts is increased, thus the probability of interaction between substrates and photogenerated active species on the semiconductor interface being increased [5,7,8,10,11].

Many authors have investigated single and coupled graphene-based semiconductor photocatalysts with the purpose of promoting the photonic efficiency of the semiconductors in the decomposition of water and air contaminants [5]. In general, it has been established that the efficiency of graphene-based semiconductor photocatalysts is higher than that of graphene-free catalysts, especially in cases of dye destruction [6]. It was shown that the percentage of graphene content with respect to the photocatalyst plays an essential role on the activity of graphene-based semiconductor photocatalysts. In most cases, a high content of graphene oxide leads to photon scattering and blocking the active sites of the semiconductor photocatalysts [5,12]. So far, the promoting effect of noble metals (gold in particular) on the TiO<sub>2</sub>/GR system efficiency has received little attention in the literature.

This work compares the catalytic activities of TiO<sub>2</sub>, Au/TiO<sub>2</sub>, and corresponding composite materials with reduced graphene oxide in the photocatalytic oxidation of 4-chlorophenol under UV light irradiation. The investigation was carried out using an optimal graphene oxide to semiconductor ratio reported in the literature [13]. A

\*) To whom all correspondence should be sent:

E-mail: iliev@ic.bas.bg

principal aim of this study was to elucidate the effect of GR presence in composite Au/TiO<sub>2</sub> materials and to evaluate rate enhancement of 4-chlorophenol oxidation under UV irradiation.

## EXPERIMENTAL

### *Materials and preparation of photocatalysts*

Titanium (IV) isopropoxide (Sigma-Aldrich), hydrogen tetrachloroaurate(III), H<sub>2</sub>AuCl<sub>4</sub>·3H<sub>2</sub>O (Sigma-Aldrich), and graphene oxide (Grapenea) were used as starting reagents for photocatalyst synthesis. Pollutant 4-chlorophenol (Sigma-Aldrich) was used without further purification.

TiO<sub>2</sub> and TiO<sub>2</sub>/GR photocatalytic materials were synthesised by the sol-gel method. The surface of some samples was modified by gold nanoparticles.

Composite TiO<sub>2</sub>/GO (GO to TiO<sub>2</sub> wt. ratio of 0.05) was prepared by the following procedure. Graphene oxide (87.5 ml) dispersed in water (4 mg ml<sup>-1</sup>) is slowly added dropwise for 2 h to a solution containing 26.9 ml of titanium(IV) isopropoxide dissolved in 30 ml of absolute ethanol. The process is conducted at pH=9 under vigorous stirring followed by ultrasonic dispersion. The resulting transparent colloidal suspension was aged for 30 h until xerogel formation. The obtained gel is filtered and dried at 100°C for 12 h. Further, the dried gel is thermal treated at 450°C for 3 h under argon flow. This temperature is reached at a ramping rate of 5 grad min<sup>-1</sup>. Thermally treated material is then ground in an agate mortar to obtain a fine titania-graphene powder.

Nanosized titania was prepared in a similar way without any addition of graphene oxide.

In the absence of oxygen the prepared photocatalyst samples were modified by nanosized gold particles (0.5 wt.%) by using the photoreduction method [3] at medium pH=7. H<sub>2</sub>AuCl<sub>4</sub>·3H<sub>2</sub>O was used as a precursor at a particular concentration to give 0.5 wt.% Au on the support. A 4-W capacity UV-C lamp (Philips, TUV 4W) was used as the light source to reduce Au<sup>3+</sup> into its metallic state Au<sup>0</sup>. This amount of noble metal was selected based on previous investigations, which reported to be optimal [3,14].

### *Photocatalyst characterisation*

BET specific surface area of the samples was measured by nitrogen adsorption from N<sub>2</sub>+He mixture at the liquid nitrogen boiling temperature using a Micromeritics FlowSorb II 2300 apparatus based on adsorption data in the partial pressure (P/P<sub>0</sub>) range of 0.05–0.35.

4-Chlorophenol adsorption on TiO<sub>2</sub>, TiO<sub>2</sub>/GR, and gold-modified semiconductor materials was

measured at pH=4 in the dark. In each experimental run, 350 mg of photocatalytic material were added to 350 ml of aqueous 4-chlorophenol solution (4×10<sup>-3</sup> mol L<sup>-1</sup>). The suspension was then magnetically stirred for 60 min at 20°C in the dark and in the absence of oxygen to attain adsorption-desorption equilibrium [15]. Afterwards the photocatalytic material was separated by filtration (Whatman, Grade 42). A Shimadzu VCSH total organic carbon (TOC) analyser was used to measure the remaining 4-chlorophenol concentration in the filtrate.

A X-ray Bruker D8 Advance diffractometer with Cu-K $\alpha$  radiation and LynxEye detector was applied to study the crystal phase of the synthesised samples.

A JEOL JEM 2100 high resolution scanning transmission electron microscope was applied to study surface morphology and to measure particle size of the synthesised TiO<sub>2</sub> and TiO<sub>2</sub>/GR samples as well as Au nanoparticle size distribution of the gold-promoted photocatalysts. These results were acquired by measuring 100 particles in each sample.

X-ray photoelectron spectroscopy (XPS) measurements were carried out using an ESCALAB Mk II (VG Scientific Ltd.) electron spectrometer under base vacuum of 10<sup>-8</sup> Pa. XPS spectra were recorded using an Mg K $\alpha$  excitation source with photon energy of 1253.6 eV. The carbon 1s line of binding energy of 284.8 eV was used to calibrate the binding-energy scale of the unit.

### *Photocatalytic experiments*

Photodegradation of 4-chlorophenol was studied in a semi-batch photoreactor containing aqueous suspensions of the semiconductor materials at a content of 1 g L<sup>-1</sup>. A constant temperature of 20°C in the reaction vessel was realised. Before catalytic measurements, each sample was dispersed in water by ultrasonic treatment for 20 min. Then the catalyst was placed into the reactor vessel equipped with a magnetic stirrer. Next, 4-chlorophenol from a stock solution was added to achieve an initial concentration of 4×10<sup>-3</sup> mol L<sup>-1</sup> that is equivalent to 290 ppm TOC. The initial volume of the irradiated reaction mixture was 350 ml. During the photocatalytic process, oxygen was bubbled continuously at a flow rate of 12 L h<sup>-1</sup>. The pH of the liquid phase of the suspensions was adjusted to four by adding a buffer solution (Fixanal, Fluka).

The photoreactor was equipped with a 9-W UV lamp (Philips PL-S 2P) for UV-A irradiation ( $\lambda \approx 365$  nm). Photon flux in the UV light region at the external wall of the quartz tube was 10 mW cm<sup>-2</sup> (UV-A) as measured by a microprocessor-controlled radiometer (Cole Parmer, 97503-00). Samples collected during the dark period and during

irradiation were filtered and, as described above, the degree of mineralisation of 4-chlorophenol was assessed by means of a TOC analyser.

## RESULTS AND DISCUSSION

### Catalyst characterisation

Studies [16–18] have proved that catalyst specific surface area, degree of crystallinity, and metal nanoparticle size on the metal oxide surface are factors that can affect significantly the efficiency of photodestruction of water contaminants. In the case of graphene-based semiconductor photocatalysts, pollutant adsorption onto composite catalysts has an essential effect on photocatalytic destruction efficiency in the aqueous phase [5,7,8,10,11].

Regardless of graphene high theoretical specific surface area (2600 m<sup>2</sup> g<sup>-1</sup>) [19], GR composites with

photocatalytic materials demonstrated lower values (Table 1). This is attributed to occurring agglomeration of the photocatalytic materials and changes in pore size distribution during graphene oxide reduction [20,21]. Compared to unmodified samples, TiO<sub>2</sub>/GR surface area was increased by 21%, whereas the Au/TiO<sub>2</sub>/GR sample manifested an increase of 23%. The gold-modified materials, Au/TiO<sub>2</sub> and Au/TiO<sub>2</sub>/GR (0.5 wt.% Au<sup>0</sup>), showed a negligible change of the specific surface area compared to the parent gold-free samples (Table 1), which is in accordance with results reported by other authors [3,15]. Small changes in surface area might be due to blocking of defect sites on the surface and penetration of finely divided gold particles into catalyst pores.

**Table 1.** Physical properties of the photocatalyst samples and pseudo-first order apparent reaction rate constants ( $k_{app}$ )

Sample	BET area <sup>a</sup> (m <sup>2</sup> g <sup>-1</sup> ) ±2%	Average gold particle size <sup>b</sup> (nm) ±10%	4-Chlorophenol adsorption (μmol gcat <sup>-1</sup> ) ±2%	$k_{app}$ (λ=365 nm) (min <sup>-1</sup> ) ±5%
TiO <sub>2</sub>	140	–	280	0.0025
TiO <sub>2</sub> /GR	170	–	540	0.0051
Au/TiO <sub>2</sub>	134	7.2	250	0.0056
Au/TiO <sub>2</sub> /GR	165	7.4	450	0.0098

<sup>a</sup> determined from N<sub>2</sub> adsorption isotherms

<sup>b</sup> determined from TEM images

4-Chlorophenol adsorption in the dark was considerably enhanced upon formation of graphene composites with TiO<sub>2</sub> and Au/TiO<sub>2</sub>, namely, 1.9 and 1.8 times on TiO<sub>2</sub>/GR and Au/TiO<sub>2</sub>/GR, respectively (Table 1). The increase in sample equilibrium adsorption capacity with respect to 4-chlorophenol is due to π-π interactions and formation of hydrogen bonds between 4-chlorophenol and graphene, the local concentration of the pollutant around the investigated photocatalysts being also increased [5,11]. On sample doping by gold the adsorption of 4-chlorophenol was decreased by 12–20% regarding undoped metal oxides (Table 1). This effect has been associated with reduction of the titania or titania/graphene external surface area that is available for adsorption of 4-chlorophenol [22].

An XRD pattern of Au/TiO<sub>2</sub>/GR is shown in Figure 1. A thermally treated sample exhibited only diffraction peaks due to anatase-phase titania (PDF # 841284). Because of low content no XRD diffraction peaks of gold (0.5 wt.%) were registered with the latter sample.

TEM micrographs of GR and composite photocatalytic materials are presented in Figure 2. TEM analysis of the samples showed that the photocatalytic materials are located on graphene surface (Fig. 2b). The average size of the titania

nanoparticles prepared by the sol-gel method was 20 nm, whereas those of the gold particles on Au/TiO<sub>2</sub> and Au/TiO<sub>2</sub>/GR were 7.2 and 7.4 nm, accordingly (Table 1). Such a small difference in gold particle sizes was insignificant as being within experimental error.

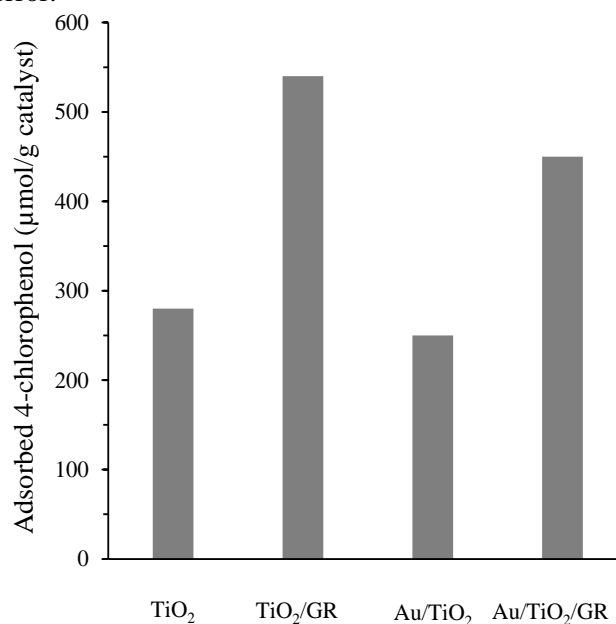


**Fig. 1.** Total amount of 4-chlorophenol adsorbed on the photocatalysts at pH 4 in the dark.

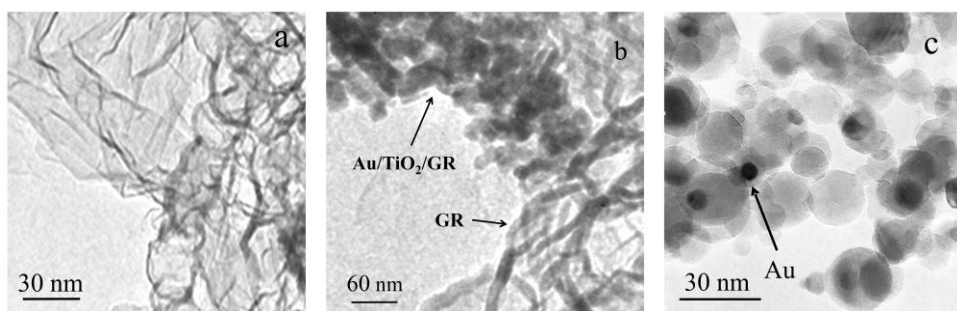


**Fig. 2.** TEM images: (a) graphene; (b) Au/TiO<sub>2</sub>/graphene; (c) Au nanoparticles in Au/TiO<sub>2</sub>/graphene.

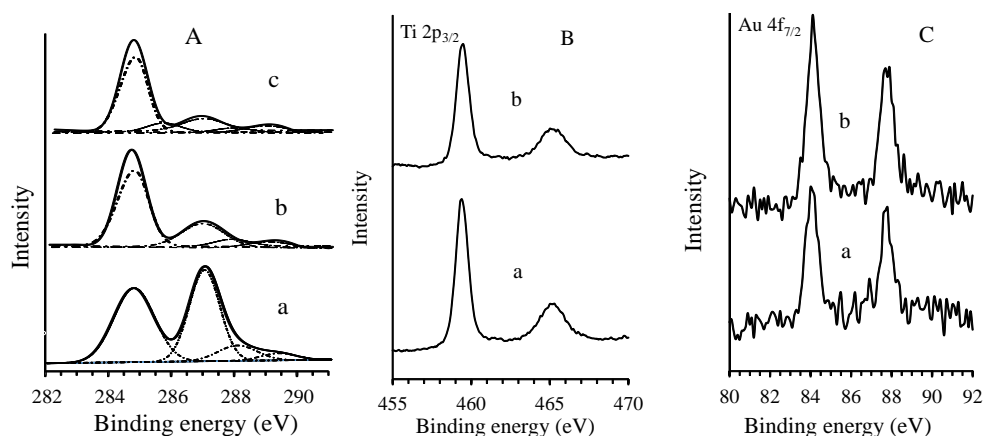


**Fig. 3.** XPS spectra: A – 1 Cs, (a) graphene oxide, (b) TiO<sub>2</sub>/graphene, (c) Au/TiO<sub>2</sub>/graphene; B – Ti 3p: (a) Au/TiO<sub>2</sub>, (b) Au/TiO<sub>2</sub>/graphene; C – Au 4f : (a) Au/TiO<sub>2</sub>, (b) Au/TiO<sub>2</sub>/graphene.

XPS spectra of graphene oxide, graphene, and composite photocatalytic materials are displayed in Figure 3. Figure 3A shows the C 1s spectra of graphene oxide, TiO<sub>2</sub>/GR, and Au/TiO<sub>2</sub>/GR samples. For GO, Fig. 3A (a), four different peaks centred at 284.6, 286.6, 287.8, and 289.0 eV were found, which are related to C=C/C–C bonds in aromatic rings, C–O (epoxy and alkoxy), C=O, and COOH groups, respectively [19]. After thermal treating of the TiO<sub>2</sub>/GO composite at 450°C (Fig. 3A (b)), the intensities of all C 1s peaks of the carbons bonded to oxygen, especially the peak of C–O (epoxy and alkoxy), decreased dramatically because of partial thermal reduction of the graphene oxide to graphene [23]. In contrast to TiO<sub>2</sub>/GR, the Au/TiO<sub>2</sub>/GR sample gave rise to another low intensity C 1s peak at a binding energy of 285.6 eV (Fig. 3A (c)), which indicates an admixture of graphene oxide and entities containing carbon atoms of sp<sup>3</sup> configuration. Most likely, this peak is due to partial destruction of the graphene caused by HO• radicals that are generated upon TiO<sub>2</sub>/GR doping as described above for the photoreduction of the gold precursor. Graphene destruction in aqueous media by HO• radicals generated upon irradiation with UV light over titania surface has already been described in the literature [24].

Neither differences in Ti 2p<sub>3/2</sub> binding energy nor peak broadening in the XPS spectra of TiO<sub>2</sub>,

TiO<sub>2</sub>/GR, and Au/TiO<sub>2</sub>/GR were registered (Fig. 3B) which indicate very weak interactions between titania and graphene.

The binding energies of the Au 4f<sub>5/2</sub> and Au 4f<sub>7/2</sub> peaks positioned at 87.6 and 83.9 eV, respectively, of gold-modified titania and TiO<sub>2</sub>/GR demonstrate that superficially attached gold was completely reduced to metallic Au<sup>0</sup>. In the presence of graphene, no other additional XPS peaks were registered or no broadening of the existing lines was observed (Fig. 3C).

#### Photocatalytic activity

4-Chlorophenol is one of the most used model pollutants for evaluation of the photocatalytic activity of metal oxide catalysts in aqueous solution. The photocatalytic degradation process of 4-chlorophenol in aqueous solution can be interpreted based on the Langmuir-Hinshelwood kinetic model. Under the applied experimental conditions of low 4-chlorophenol concentration and constant UV light flux, the Langmuir kinetic expression [25] can be reduced to a pseudo-first order kinetics equation with respect to the pollutant:

$$\ln C_0/C = k_{app} t, \quad (1)$$

where  $k_{app} = k_r K$ , and  $k_r$  is the rate constant of the limiting step of the reaction at a maximum coverage under the applied experimental conditions,  $K$  is 4-

chlorophenol adsorption-desorption equilibrium constant,  $C_0$  is the initial concentration of 4-chlorophenol, and  $C$  is 4-chlorophenol concentration at a given moment in the course of the photocatalytic reaction. Figure 4 shows a plot of  $\ln C_0/C$  vs. time for the experiments of 4-chlorophenol photocatalytic decomposition. The photocatalytic rates are, therefore, dependent on 4-chlorophenol coverage on the catalysts and 4-chlorophenol concentration.

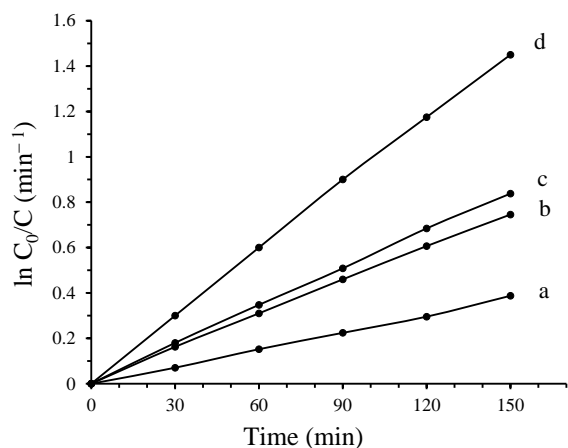


**Fig. 4.** Pseudo-first order kinetics of 4-chlorophenol photocatalytic degradation ( $4 \times 10^{-3}$  mol L<sup>-1</sup>) at pH=4 by irradiation with UV light in the presence of: (a) TiO<sub>2</sub>, (b) TiO<sub>2</sub>/GR, (c) Au/TiO<sub>2</sub>, (d) Au/TiO<sub>2</sub>/GR.

Values of the apparent rate constants of 4-chlorophenol photocatalytic mineralisation over suspended semiconductor materials irradiated with UV-A light are listed in Table 1. The rate constants with UV-A irradiation decrease in the following order: Au/TiO<sub>2</sub>/GR > Au/TiO<sub>2</sub> > TiO<sub>2</sub>/GR > TiO<sub>2</sub> (Fig. 4). Under UV-A irradiation the TiO<sub>2</sub>/GR composite photocatalyst showed a 2-fold increase in the rate of 4-chlorophenol mineralisation compared with the titania photocatalyst. On the other hand, the rate constant values of 4-chlorophenol destruction were increased approximately two times on doping the photocatalysts with gold nanoparticles (Table 1).

Regarding the graphene-free photocatalysts, two principal factors have influence on the increased rate constants of 4-chlorophenol destruction over TiO<sub>2</sub>/GR and Au/TiO<sub>2</sub>/GR. Considering 4-chlorophenol, a higher adsorption capacity of the GR photocatalysts (Fig. 1) is accompanied by enhanced local concentration of the pollutant around the investigated photocatalysts, which facilitates the interaction between photogenerated active species and 4-chlorophenol at TiO<sub>2</sub>/GR and Au/TiO<sub>2</sub>/GR interfaces. A correlation exists between the higher adsorption capacity of the GR composites and their photocatalytic activity (Table 1). On the other hand, it is known that on depositing semiconductor nanoparticles on graphene sheets, the graphene acts

like an electron acceptor by inducing charge carrier separation in the photoexcited semiconductor catalyst [8]. Charge carrier separation also favours an increased activity of the graphene-based semiconductor photocatalysts.

The rate constants of 4-chlorophenol destruction were increased in all cases of photocatalyst modification with gold nanoparticles (Table 1). The effect of gold content and Au nanoparticle size on the photocatalytic activity of modified semiconductor materials under UV and visible light irradiation has been reported in previous works from this laboratory [3,15,17,22]. On depositing noble metal nanoparticles onto the surface of titania and TiO<sub>2</sub>/GR an increase of the quantum yield of the photodestruction reaction of the studied pollutant has been observed. It is due to enhanced separation of electrons and holes and to a higher rate of HO<sup>•</sup> radical formation mainly on the valence band and on the conduction band in the photoexcited semiconductors [26]. Noble metal nanoparticles are highly effective traps for electrons owing to the formation of a Schottky barrier at the metal-semiconductor interface. The Au/TiO<sub>2</sub>/GR system was particularly efficient upon irradiation with UV light and the rate constant of 4-chlorophenol decomposition was approximately 3.9 times higher than that with pure titania (Table 1). In this case, the increased rate constant of 4-chlorophenol decomposition is owing to an enhanced local concentration of the pollutant around the investigated photocatalyst and due to simultaneous charge carrier separation over both gold nanoparticles and graphene (Fig. 5).

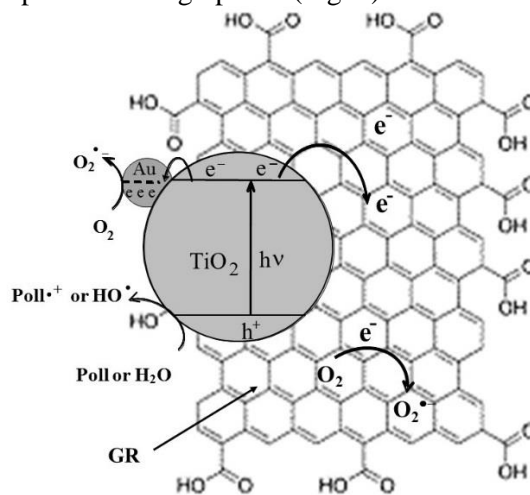


**Fig. 5.** Schematic presentation of charge carrier separation in the photoexcited Au/TiO<sub>2</sub>/GR photocatalyst.

## CONCLUSIONS

4-Chlorophenol photodestruction catalysed by TiO<sub>2</sub>/GR showed a higher rate constant in comparison with titania counterpart which could be

attributed to an enhanced local concentration of the pollutant around the investigated photocatalysts and to an increased probability for interaction between the photogenerated active species and 4-chlorophenol at TiO<sub>2</sub>/GR interface.

In the case of deposited nanosized gold particles (0.5 wt.%) on the surface of the catalysts the higher rate of photocatalytic destruction of 4-chlorophenol is owing to an efficient charge carrier separation, an increase in the lifetime of the excitons, and enhancement of the effectiveness of the interphase charge transfer to adsorbed pollutant molecules. Charge carrier separation was especially efficient during irradiation of the Au/TiO<sub>2</sub>/GR photocatalyst with UV light. In this case, the rate constant of 4-chlorophenol decomposition over the latter was approximately 3.9 times higher than that with pure titania.

**Acknowledgement:** The authors gratefully acknowledge financial support by the Bulgarian Science Fund (Contract DFNI-T02/16).

#### REFERENCES

1. K. Nakata, A. Fujishima, *J. Photochem. Photobiol. C: Photochem. Rev.*, **13**, 169 (2012).
2. H. Park, Y. Park, W. Kim, W. Choi, *J. Photochem. Photobiol. C: Photochem. Rev.*, **15**, 1 (2013).
3. V. Iliev, D. Tomova, S. Rakovsky, A. Eliyas, G. Li Puma, *J. Mol. Catal. A: Chem.*, **327**, 51 (2010).
4. A. Ayati, A. Ahmadvpour, F.F. Bamoharram, B. Tanhaei, M. Mänttari, M. Sillanpää, *Chemosphere*, **107**, 163 (2014).
5. R.K. Upadhyay, N. Soin, S.S. Roy, *RSC Adv.*, **4**, 3823 (2014).
6. S. Chowdhury, R. Balasubramanian, *Appl. Catal. B: Environ.*, **160–161**, 307 (2014).
7. N. Zhang, Y. Zhang, Y.-J. Xu, *Nanoscale*, **4**, 5792 (2012).
8. Q. Xiang, J. Yu, M. Jaroniec, *Chem. Soc. Rev.*, **41**, 782 (2012).
9. A.S.A. Shalaby, A.D. Staneva, L.I. Aleksandrov, R.S. Iordanova, Y.B. Dimitriev, *Bulg. Chem. Commun.*, **48**, 38 (2016).
10. Y.H. Ng, I. V. Lightcap, K. Goodwin, M. Matsumura, P.V. Kamat, *J. Phys. Chem. Lett.*, **1**, 2222 (2010).
11. J. Liu, Z. Wang, L. Liu, W. Chen, *Phys. Chem. Chem. Phys.*, **13**, 13216 (2011).
12. S. Morales-Torres, L. M. Pastrana-Martínez, J. L. Figueiredo, J. L. Faria, A.M.T. Silva, *Environ. Sci. Pollut. Res.*, **19**, 3676 (2012).
13. S. Ghasemi, S. Rahman Setayesh, A. Habibi-Yangjeh, M.R. Hormozi-Nezhad, M.R. Gholami, *J. Hazard. Mater.*, **199–200**, 170 (2012).
14. B. Cojocaru, S. Neatu, E. Sacaliuc-Parvulescu, F. Levy, V.I. Parvulescu, H. Garcia, *Appl. Catal. B: Environ.*, **107**, 140 (2011).
15. M. Daous, V. Iliev, L. Petrov, *J. Mol. Catal. A: Chem.*, **392**, 194 (2014).
16. C.G. Granqvist, *Sol. Energy Mater. Sol. Cells*, **91**, 1529 (2007).
17. V. Iliev, D. Tomova, L. Bilyarska, G. Tyuliev, *J. Mol. Catal. A: Chem.*, **263**, 32 (2007).
18. A. Orlov, D.A. Jefferson, N. Macleod, R.M. Lambert, *Catal. Lett.*, **92**, 41 (2004).
19. O. Akhavan, E. Ghaderi, *J. Phys. Chem. C*, **113**, 20214 (2009).
20. H. Adamu, P. Dubey, J.A. Anderson, *Chem. Eng. J.*, **284**, 380 (2016).
21. Md.S.A. Sher Shah, A R. Park, K. Zhang, J.H. Park, P.J. Yoo, *ACS Appl. Mater. Interfaces*, **4**, 3893 (2012).
22. V. Iliev, D. Tomova, R. Todorovska, D. Oliver, L. Petrov, D. Todorovsky, M. Uzunova – Bujnova, *Appl. Catal. A: General*, **313**, 115 (2006).
23. S. Pei, H.-M. Cheng, *Carbon*, **50**, 3210 (2012).
24. J.G. Radich, A.L. Krenselewski, J. Zhu, P.V. Kamat, *Chem. Mater.*, **26**, 4662 (2014).
25. N. Serpone, A. Salinaro, A. Emeline, V. Ryabchuk, *J. Photochem. Photobiol. A: Chem.*, **130**, 83 (2000).
26. V. Subramanian, E.E. Wolf, P.V. Kamat, *Langmuir*, **19**, 469 (2003).

ПРОМОТИРАНЕ НА СКОРОСТТА НА ОКИСЛИТЕЛНО ОТСТРАНЯВАНЕ НА  
4-ХЛОРФЕНОЛ ВЪРХУ ЗЛАТО-ДОТИРАНИ TiO<sub>2</sub>/ГРАФЕН ФОТОКАТАЛИЗАТОРИ  
ПРИ ОБЛЪЧВАНЕ С УЛТРАВИОЛЕТОВА СВЕТЛИНА

В. И. Илиев\*, Д. В. Томова, В. Ф. Георгиев, С. К. Раковски

*Институт по катализ, Българска академия на науките, 1113 София, България*

Постъпила на 9 ноември, 2016 г.; коригирана на 23 март, 2017 г.

Фотоокислението на 4-хлорфенол, катализирано от наноразмерни TiO<sub>2</sub>, Au/TiO<sub>2</sub> и от съответните композитни материали с редуциран графенов оксид (GR) са изследвани при облъчване с ултравиолетова светлина. XPS и TEM методи са използвани за охарактеризиране на получените фотокатализатори. Средният размер на наночастиците от TiO<sub>2</sub> получен по зол-гел метода е 20 nm. TiO<sub>2</sub> и Au/TiO<sub>2</sub> са разпределени на случаен принцип на повърхността на нанолестовете от графен. Средният размер на Au наночастици в модифицираните TiO<sub>2</sub> фотокатализатори е  $\approx 7$  nm. XPS измерванията потвърждават частичната термо- или фото-редукция на графеновия оксид до графен. Скоростните константи на фотоокисление на 4-хлорфенол катализирани от изследваните образци следват реда: Au/TiO<sub>2</sub>/GR > Au/TiO<sub>2</sub> > TiO<sub>2</sub>/GR > TiO<sub>2</sub>. Скоростната константа на деструкция на 4-хлорфенол катализирана от Au/TiO<sub>2</sub>/GR композита е приблизително 3.9 пъти по-висока от тази регистрирана с чист TiO<sub>2</sub>. Повишаването на активността на Au/TiO<sub>2</sub>/GR, Au/TiO<sub>2</sub> и TiO<sub>2</sub>/GR фотокатализаторите е резултат от по-ефективното разделяне на носителите на заряди в генерираните от светлина електрон-дупка двойки в полупроводника TiO<sub>2</sub>. Това благоприятства допълнителното генериране на OH• радикали върху валентната зона на TiO<sub>2</sub>.